The Molecular Mechanisms and Gene Expression Profiling for Shikonin-induced Apoptotic and Necroptotic Cell Death in U937 cells

Jin-Lan Piao

Department of Radiological Sciences

Graduate School of Medicine and Pharmaceutical Sciences for Education

(Ph.D. Program)

University of Toyama

2014

Contents

1. Summary

Shikonin (SHK), a natural naphthoquinone derived from the Chinese medical herb *Lithospermum erythrorhizon*, induces both apoptosis and necroptosis in several cancer cell lines. However, the detailed molecular mechanisms involved in the initiation of cell death are still unclear. In the present study, caspase-dependent apoptosis was induced by SHK treatment at 1 μM after 6 h in U937 cells, with increase in DNA fragmentation, generation of intracellular reactive oxygen species (ROS), fraction of cells with low mitochondrial membrane potential (MMP), and in the expression of BH3 only proteins Noxa and tBid. Interestingly, caspase-independent cell death was also detected with SHK treatment at 10 μM, observed as increase in SYTOX® Green staining and release of lactate dehydrogenase (LDH). Necrostatin-1 (Nec-1) completely inhibited the SHK-induced leakage of LDH and SYTOX® Green staining. Cell permeable exogenous glutathione (GSH) completely inhibited 1 μM SHK-induced apoptosis and converted 10 μM SHK-induced necroptosis to apoptosis. Gene expression profiling revealed that 353 genes were found to be significantly regulated by 1 μM and 85 genes by 10 μM of SHK treatment, respectively. Among these genes, the transcription factor 3 (ATF3) and DNA-damage-inducible transcript 3 (DDIT3) were highly expressed at 1 μM of SHK treatment, while tumor necrosis factor (TNF) expression mainly increased at 10 μM treatment. These findings provide novel information for the molecular mechanism of SHK-induced apoptosis and necroptosis.

2. Introduction

Shikonin (SHK) is a chemical compound isolated from the root of *Lithospermum erythrorhizon*. SHK is well known to have antibacterial [1], anti-human immunodeficiency virus [2], and anti-inflammatory activity [3]. It has been reported that SHK has significant potential against various cancer cell lines, by inhibiting cell growth and inducing cell death [4]. SHK can induce apoptosis by increasing the production of intracellular reactive oxygen species (ROS) [5, 6]. Recently, it has been reported that SHK induces necroptosis and that this mode of cell death could be blocked and converted into apoptosis by Necrostatin-1 (Nec-1) [7].

Apoptosis, a genetically programmed cell death, was originally defined in terms of characteristic changes in cell morphology that include plasma membrane blebbing, cell shrinkage, nuclear fragmentation, chromatin condensation, and chromosomal DNA fragmentation [8]. Apoptosis plays pivotal roles in the host defense and suppression of oncogenesis; dysregulation of apoptosis leads to pathogenesis of several diseases ranging from cancer and auto-immunity to degenerative disorders [9, 10]. Therefore, apoptosis was extensively investigated in the last decades. There are two pathways for mammalian apoptosis. The 'extrinsic' pathway is triggered by engagement of cell surface 'death receptors' of the tumor necrosis factor receptor (TNFR) family with their ligands [11]. The 'intrinsic' (or mitochondrial) pathway is activated following the release of cytochrome c into the cytoplasm; the event regulated by interactions between proteins related to Bcl-2 family [12].

On the other hand, necrosis is morphologically characterized by rounding of the cells, increase in the cell volume, organelle swelling, plasma membrane rupture and lack of inter-nucleosomal DNA fragmentation. In contrast to apoptosis, it is considered as a passive form of cell death without intricate regulatory mechanisms [13]. However, recently it has been proposed that necroptosis is a form of programmed cell death, which is distinct from apoptosis, but characterized by necrotic cell death morphology [14]. In addition, Nec-1 has been identified as a specific and potent small-molecule that

specifically inhibits necroptosis, without any effect on apoptosis. Nec-l blocks receptor-interacting protein 1 (RIP1) is a critical molecule in necroptosis, and has been used as an operational definition of necroptosis [15]. The activation of RIP1 in response to the ligation of TNFR and the formation of a RIP1-RIP3 complex (necrosome) is the hallmark of necroptosis [16, 17].

Current DNA microarray technology provides a way to view the expression profiles of many thousands of genes. In addition, technologies for pathway analysis now allow mapping of gene-expression data by fitting them into relevant pathway maps based on their functional annotation and known molecular interaction.

SHK has been used widely as a model compound for apoptosis or necroptois. However, the detailed molecular mechanisms and the genes involved in SHK-induced cell death are still not fully understood. The present study aims to clarify the molecular mechanisms of SHK involved in initiating different types of cell death, namely; apoptosis and necroptosis. Furthermore, we examined gene expression patterns in human myelomonocytic lymphoma U937 cells using a GeneChip® analyzing system. The functional relationships among candidate genes were examined using Ingenuity Pathway Analysis tools for better understanding the mechanisms of SHK- induced cell death.

3. Materials and methods

3.1. Reagents

SHK, Tetramethylrhodamine methyl ester (TMRM) and glutathione (GSH) were purchased from Wako (Osaka, Japan). Nec-1 and glutathione monoethyl ester (GSH-MEE) were obtained from Santa Cruz Biotechnology, Inc. (Santa Cruz, CA). SYTOX® Green Nucleic Acid Stain (Molecular Probes, Inc. Eugene, OR) was purchased from Invitrogen. Hydroxyphenyl fluorescein (HPF) was purchased from Sekisui Medical. Z-VAD-FMK was purchased from Protein Institute (Osaka, Japan). Anti-TNF-α, anti-DDIT3, secondary HRP-conjugated anti-mouse or anti-rabbit IgGs were purchased from Cell Signaling Technology (Beverly, MA). Anti-ATF3 was purchased from Calbiochem (CA, USA).

3.2. Cell line and culture

The human lymphoma U937 cells (Human Sciences Research Resource Bank, Tokyo, Japan) were cultured in RPMI 1640 medium containing 10% heat-inactivated fetal bovine serum (FBS) at 37 °C in humidified air with 5% CO_2.

3.3. Morphological cell death assay

Hoechst staining was performed to identify cells with nuclear changes typical of apoptotic cell death [18]. The cells were harvested at 6 h after treatment with SHK and stained with 2 μg/ml of Hoechst 33342 (Sigma), for 10 min in the dark at 4 °C. The nuclear morphology was observed under a fluorescence microscope. Apoptotic cells were undergoing nuclear condensation and fragmentation was counted within a total of at least 500 cells per sample in random areas.

SYTOX® Green is a membrane-impermeant dye excluded from cells when the plasma membrane is intact. In dying cells with increased plasma membrane permeability, nuclear fluorescence becomes apparent. To determine the mode of cell death, U937 cells were harvested at 6 h after treatment with SHK. The samples were

washed with phosphate buffered saline (PBS) and incubated for 15 min with 5 μM of SYTOX® Green dye, and morphological changes in the nuclei were examined by fluorescence microscope.

3.4. DNA fragmentation assay

The quantitative DNA fragmentation assay was carried out according to the method of Sellins and Cohen [19] with minor modifications. U937 cells were treated with SHK in a dose-dependent manner. After 6 h, the cells were harvested and lysed with 200 μM of lysis buffer (1 mM EDTA, 0.2% Triton X-100, 10 mM Tris–HCI, pH 7.5) and centrifuged at 13,000 × g for 10 min at 4 °C. Subsequently, each DNA sample in the supernatant and the resulting pellet were precipitated in 12.5% trichloroacetic acid (TCA) at 4 °C, and quantified using the diphenylamine reagent after hydrolysis in 5% TCA at 90 °C for 20 min. The percentage of fragmented DNA for each sample was calculated as the amount of DNA in the supernatant divided by the total DNA for that sample (supernatant plus pellet).

U937 cells were pretreated with the antioxidant agents GSH-MEE 1 mM or GSH 5 mM for 1 h and then treated with SHK in a dose-dependent manner. After 6 h incubation, DNA fragmentation assay was performed.

3.5. Cytotoxicity assay

To evaluate SHK-induced cytotoxicity in U937 cells by lactate dehydrogenase (LDH) assay, the release of LDH from cells into the culture medium was measured in a dose- and time-dependent manner using the LDH Cytotoxicity Detection Kit (Takara Bio, Shiga, Japan) according to the manufacturer´s instructions. Cytotoxicity was expressed in percentage, taking the activity of LDH liberated from lysed cells as 100%.

3.6. Analysis of mitochondrial membrane potential (MMP)

The cationic fluorophore, TMRM, accumulates in mitochondria in response to MMP and is released upon loss of MMP [20]. The samples were centrifuged at 500 x g

for 5 min. The resulting pellets (1×10^6 cells/sample) were stained with 10 nM of TMRM for 15 min at 37 °C in PBS. The Percentage of cells showing low MMP was measured by flow cytometry.

3.7. Assessment of intracellular ROS

To measure intracellular ROS we used the HPF. HPF is a suitable probe for detecting the generation of intracellular ROS including •OH and ONOO–. U937 cells were treated with 1 μM of SHK in a time-dependent manner. Briefly, the samples were centrifuged at 500 x g for 5 min. The resulting pellets (1×10^6 cells/sample) were loaded with 5 μM of HPF for 15 min at 37 °C. The fluorescence emission was measured by flow cytometry.

3.8. Western blot analysis

The cells were collected and washed with cold PBS. Cells were lysed in a RIPA buffer (150 mM NaCI, 1% Nonidet P-40 (v/v), 1% sodium deoxycholate, 0.05% SDS, 1 μg/ml each of aprotinin, pepstatin, and leupeptin, 1 mM phenylmethl sulfonyl fluoride, 50 mM Tris–HCI, pH 7.2) for 20 min on ice. After brief sonication, the lysates were centrifuged at 13,000 x g for 10 min at 4 °C, and protein concentrations in the supernatant were measured using a Bio-Rad Protein Assay kit (Bio-Rad, Hercules, CA). Western blot analysis of Bcl-2 family proteins, caspase-3, caspase-8, cytochrome c (Santa Cruz, CA) and β-actin (Sigma) were performed using specific monoclonal or polyclonal antibodies. Using the secondary horseradish peroxidase (HRP) conjugated anti-rabbit and anti-mouse IgGs, protein signals were detected using an ECL kit (Amersham Biosciences, Buckingham-shire, UK) [21]. For the assay of the release of cytochrome c from mitochondria to cytosol, the cytosolic fraction was prepared as follows. The cells were collected, washed with PBS, and suspended in 300 μl of extraction buffer (210 mM D-mannitol, 70 mM sucrose, 5 mM EDTA, 1 μg/ml each of aprotinin, pepstain, and leupeptin, 1 mM PMSF, 10 mM HEPES-KOH, pH 7.4). After 5 min incubation on ice, the cells were homogenized and centrifuged at 1500 x g for 5

min at 4 °C to remove nuclei and debris. Then, the supernatant was centrifuged at 105,000 x g for 30 min at 4 °C. The resulting supernatant was used as the soluble cytosolic fraction.

3.9. RNA isolation

Total RNA was extracted from cells using a FastPure® RNA kit (Takara Bio, Shiga, Japan) and treated with RNase-free DNase I for 15 min at room temperature to remove residual genomic DNA.

3.10. High-density oligonucleotide microarray and computational gene expression analysis

Gene expression was analyzed using a GeneChip® system with a Human Genome U133-plus 2.0 array (Affymetrix, Santa Clara, CA) spotted with 54,675 probe sets. Samples for array hybridization were prepared as described in the Affymetrix GeneChip® Expression Technical Manual. Briefly, 5 μg of total RNA was used to synthesize double-stranded cDNA with a GeneChip® Expression 3´-Amplification Reagents One-Cycle cDNA synthesis kit (Affymetrix). Biotin-labeled cRNA was then synthesized from the cDNA using GeneChip® Expression 3´-Amplification Reagents for IVT labeling (Affymetrix). After fragmentation, the biotinylated cRNA was hybridized to the GeneChip array at 45 °C for 16 h. The arrays were washed, stained with streptavidin–phycoerythrin, and scanned using a probe array scanner. The scanned chip was analyzed using GeneChip Analysis Suite Software (Affymetrix). The obtained hybridization intensity data were converted into a presence or an absence call for each gene, and changes in gene expression level between experiments were detected by comparison analysis. The data were further analyzed using Gene-Spring software (Silicon Genetics, Redwood City, CA) to extract the significant genes. To examine gene ontology, including biological processes, cellular components, molecular functions, and genetic networks, the obtained data were analyzed using Ingenuity Pathways Analysis tools (Ingenuity Systems, Mountain View, CA), a web-delivered

application that enables the identification, visualization and exploration of molecular interaction networks in gene expression data. The gene lists identified by Gene-Spring containing Affymetrix gene ID and the natural logarithm of normalized expression signal ratios from GeneChip CEL files were uploaded into the Ingenuity Pathways Analysis system. Each gene identifier was mapped to its corresponding gene object in the Ingenuity Pathways Knowledge Base. These so-called focus genes were then used as a starting point for generating biological networks [22].

3.11. Real-time quantitative polymerase chain reaction (qPCR) assay

Real-time qPCR assay was performed on a Real-Time PCR system (Mx3000p, Stratagene Japan, Tokyo, Japan) using SYBR Premix Ex Tag II (Takara Bio, Shiga, Japan) according to the manufacture's protocol. Reverse transcriptase reaction (PrimeScript® RT reagent Kit, Takara Bio) was carried out with DNase-treated total RNA using a random primer $pd(N)_6$. Real-time qPCR assay was performed using the specific primers listed in Table 1. The transcript levels of these genes were estimated from the respective standard curves. Each mRNA expression level was normalized to the mRNA expression level of glyceraldehyde-3-phosphate dehydrogenase (GAPDH) [23].

Table 1

Nucleotide sequences of primers and a TagMan probe for target genes.

Genes	Orientation	Nucleotide sequence (Position)	GeneBank accession No.
ATF3	Sense	5′-ACCTGACGCCCTTTGTCAAG-3′	AB066566
	Antisense	5′-GGCACTTTGCAGCTGCAATC-3′	
DDIT3	Sense	5′-CTCCAGATTCCAGTCAGAGC-3′	BT006691
	Antisense	5′-GCGCTCGATTTCCTGCTTGA-3′	
TNF	Sense	5′-CACTGAAAGCATGATCCGGG-3′	M10988
	Antisense	5′-GGCTGATTAGAGAGAGGTCC-3′	
GAPDH	Sense	5′-AAGGCTGGGGCTCATTTGCA-3′	NM_002046
	Antisense	5′-ATGACCTTGCCCACAGCCTT-3′	

3.12. Statistical analysis

All data are presented as mean ± standard deviation (SD) from at least three independent experiments. Significance was assessed with Student's *t*-test and was assumed for *p*-values < 0.01.

4. Results

4.1. Caspase-dependent apoptotic cell death induced by low dose SHK

To examine SHK-induced cell death, U937 cells were treated with SHK in a dose-dependent manner. After 6 h, apoptosis was induced at low doses of SHK significantly. A peak in level of apoptosis was observed at 1 μM of SHK, with DNA fragmentation over 50% (Fig. 1A).

In order to examine SHK-induced changes in U937 cells morphology, the cells were treated with 1 μM of SHK for 6 h and then collected for Hoechst staining. Typical signs of apoptosis, namely chromatin condensation and nuclear fragmentation were observed. Moreover, pretreatment with Z-VAD-FMK (a pan-caspase inhibitor) almost completely inhibited these apoptotic features (Fig. 1B).

To study the potential effects of SHK on the mitochondrial apoptotic pathway, the cells were treated with 1 μM of SHK, fraction of cells with low MMP were significantly increased in a time-dependent manner (Fig. 1C).

To examine the involvement of oxidative stress in apoptosis, the cells were treated with 1 μM of SHK time-dependently, and the intracellular ROS was monitored by flow cytometry with HPF. According to the results shown in Fig. 1D, the generation of intracellular •OH and ONOO− was significantly increased by 1 μM of SHK at 6 h.

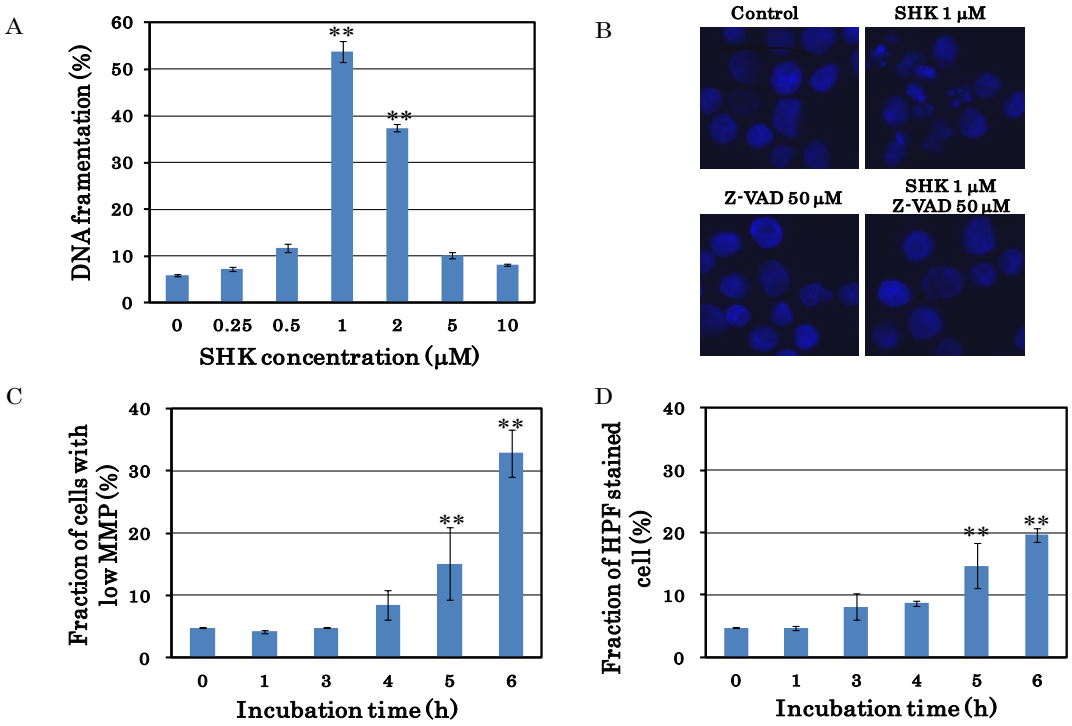

Figure 1. SHK induces apoptosis at low concentration in U937cells. (A) U937 cells were treated with SHK at indicated concentrations (0.25-10 μM) for 6 h followed by DNA fragmentation assay. (B) U937 cells were treated with 1 μM of SHK in the presence or absence of 50 μM Z-VAD-FMK for 6 h. Signs of apoptosis were detected by Hoechst staining and then examined under a fluorescence microscope at x400 magnification. (C**)** After treatment with 1 μM of SHK from 1 to 6 h, cells were stained with 10 nM of TMRM for 15 min. Loss of MMP was measured by flow cytometry. (D**)** After administration of 1 μM of SHK for the indicated time, the cells were stained with 5 μM of HPF for 15 min, the intracellular •OH and ONOO- were measured by flow cytometry. The results are presented as the means ± SD (n = 3). $^{**}p < 0.01$ denotes a mean significantly different from control.

4.2. Necroptosis induced by high concentration of SHK

Next we examined necroptosis induced by higher concentration of SHK. LDH leakage in the culture medium is an index for detecting necrosis and necroptotic program cell death due to damaged cytomembrane. Release of LDH into the culture medium was significantly increased in a dose- and time-dependent manner (Fig. 2A). Interestingly, LDH leakage with 10 μM of SHK was completely inhibited in the presence of Nec-1, but not in the presence of Z-VAD-FMK (Fig. 2B).

Further, the mode of cell death was determined by SYTOX® Green staining after treatment with SHK for 6 h. SYTOX® Green stained cells were significantly increased

by 10 μM of SHK, while no significant changes were detected in the cells treated with 1 μM of SHK. In addition, the pre-treatment with Nec-l significantly decreased the number of SYTOX® green stained cells (Fig. 2C). These results indicate that higher concentration of SHK can induce necroptosis instead of apoptosis.

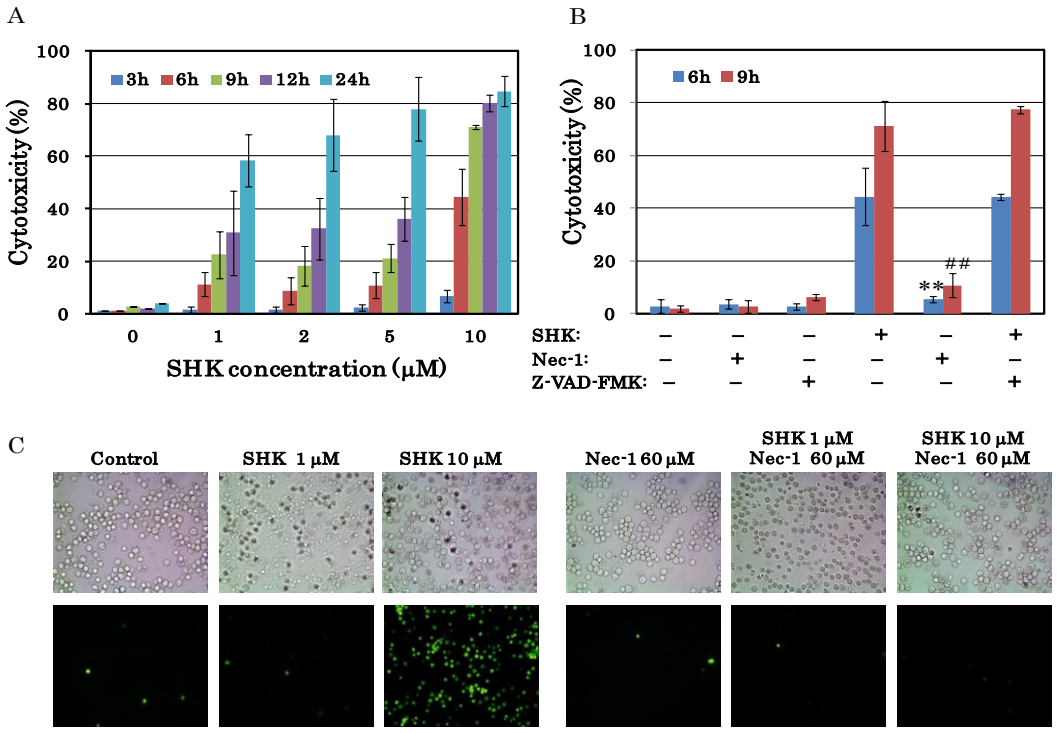

Figure 2. **SHK induces necroptosis at higher concentration and inhibited by Nec-1 in U937cells.** (A**)** LDH leakage assay was performed after the cells were treated with SHK in a dose- and time-dependent manner. The results are presented as the means ± SD (n = 3). (B**)** The cells were pretreated with 60 μM of Nec-1or 50 μM of Z-VAD-FMK for 30 min, and then treated with 10 μM of SHK for 6 h and 9 h, LDH release into the culture medium was measured. The results are presented as the means ± SD (n = 3). $^{**}p < 0.01$, compared with 10 μM of SHK for 6 h, $^{\#\#}p < 0.01$, compared with 10 μM of SHK for 9 h. (C) U937 cells were pretreated with or without 60 μM of Nec-1 for 30 min, and then treated with 1 and 10 μM of SHK for 6 h. Cell death was detected by SYTOX® Green staining and then examined under a fluorescence microscope at x200 magnification. One representative photomicrograph from three independent experiments is shown here.

4.3. The effects of GSH on the cell death induced by SHK

Pretreatment with cell membrane permeable GSH-MEE at 1 mM for 1 h significantly prevented SHK-induced apoptosis (Fig. 3A). In addition, treatment with GSH-MEE converted the 10 μM SHK-induced necroptosis to apoptosis characterized

by an increase of DNA fragmentation. Interestingly, pretreatment with cell impermeable GSH could also inhibit the apoptosis completely (Fig. 3B). Collectively, these results indicate that SHK might interact with GSH causing its depletion. Thus, oxidative stress seems to play important roles in both SHK-induced apoptosis and necroptosis.

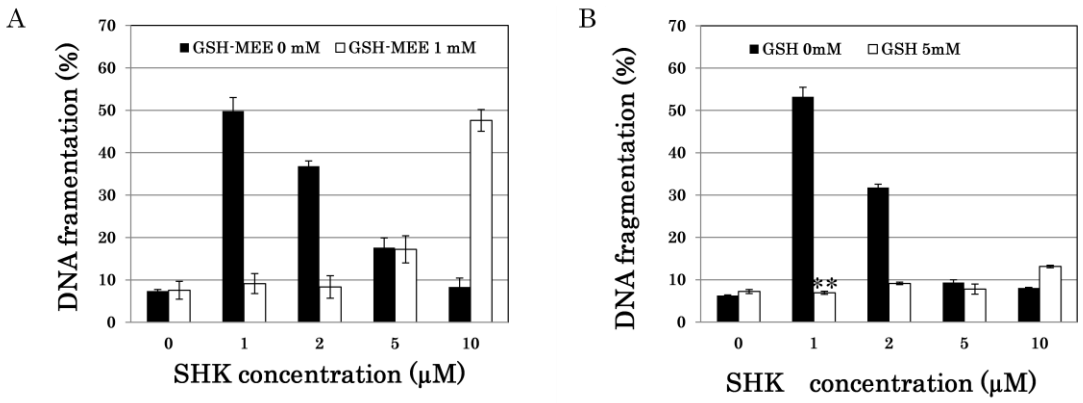

Figure 3. Effects of GSH on the cell death induced by SHK. U937 cells were pretreated with or without 1 mM of cell permeable GSH-MEE (A) or 5 mM of cell impermeable GSH (B) for 1 h, and then stimulated with SHK at indicated concentrations. DNA fragmentation assay was carried out after 6 h. The results are presented as the means ± SD (n = 3). $^{**}p < 0.01$, compared with 1 μM of SHK treatment, $^{\#\#}p < 0.01$, compared with 10 μM of SHK treatment.

4.4. Changes in the expression of apoptosis-related proteins

To determine whether MMP changes or rupture of cell membrane led to release of cytochrome c, the cells were treated with SHK in a dose-dependent manner followed by Western blotting. As shown in Fig. 4A, after 6 h incubation significant release of cytochrome c from the mitochondria to the cytosol was determined at 1 μM of SHK; the release of cytochrome c was further increased at 10 μM of SHK.

Caspase-3 activity was significantly increased at 1 μM of SHK treatment, while it was completely absent at 10 μM of SHK treatment. Here we showed that 10 μM of SHK in the presence of Nec-1 slightly increased caspase-3 activity. Therefore, these results suggest that Nec-1 also converts the necroptosis into apoptosis in U937 cells (Fig. 4B).

Western blot analysis revealed that 1 μM of SHK induced down-regulation of anti-apoptotic protein Bcl-xL, increases in cleaved form of Bid (tBid) and Noxa, while no such findings were observed with 10 μM of SHK treatment. However, in the presence of Nec-1 both concentrations showed increases in the expression of tBid and Noxa. Although Bax and Bcl-2 have been regarded as the regulators of the cytochrome c release in apoptosis, no change was observed in the expressions of both (Fig. 4C).

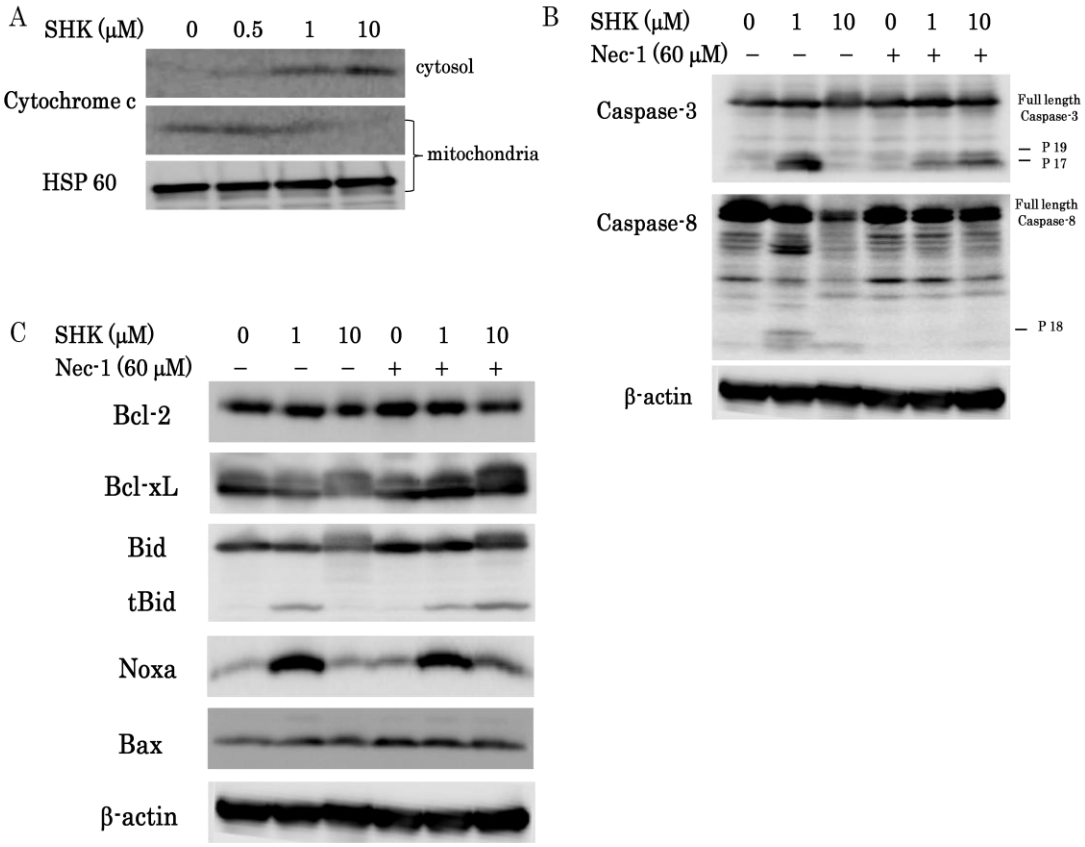

Figure 4. Changes in the expression of apoptosis-related proteins. (A**)** After treatment with SHK at the indicated concentrations for 6 h, release of cytochrome c from mitochondria to the cytosol was determined by Western blot. HSP60 was used as loading control. (B**)** The cells were pretreated with 60 μM of Nec-1 for 30 min, and then treated with 1 and 10 μM of SHK for 6 h, the activation of caspase-3; caspase-8 was determined by Western blot. (C**)** U937 cells were treated with 1 and 10 μM of SHK with or without 60 μM of Nec-1 for 6 h, expression of Bcl-2 family proteins was determined by Western blot. Representative results from three independent experiments are shown.

4.5. Identification and functional analyses of SHK responsive genes

To analyze gene-expression profiling of the cells treated with SHK, we carried out

GeneChip® analysis of cells treated with SHK 1 and 10 μM for 3 h incubation. Many probe sets were differentially expressed by ≥2.5-fold in cells treated with SHK: 353 up-regulated genes in cells treated with 1 μM treatment and 85 up-regulated genes in cells with 10 μM treatment were detected in comparison to control (Supplementary Table S1). Fifty of these up-regulated genes were common to both treatment groups.

The biologically relevant networks of the differentially expressed genes identified from the GeneChip® analysis were depicted using Ingenuity Pathway Knowledge Base. The networks contained genes related to apoptosis was up-regulated under 1 μM of SHK, including transcription factor 3 (ATF3), DNA-damage-inducible transcript3 (DDIT3), jun proto-oncogene (JUN), phorbol-12-myristate-13-acetate-induced protein 1 (PMAIP1), protein phosphatase 1 regulatory subunit 15A (PPP1R15A). However, these apoptosis promoting genes were significantly inhibited by 10 μM of SHK. In addition, BCL2-associated athanogene 3 (BAG3) and HSP-related genes such as DnaJ (Hsp40) homolog, subfamily B, member 1 (DNAJB1), heat shock 70 kDa protein 1A (HSPA1A)/heat shock 70 kDa protein 1B (HSPA1B) also elevated at 1 μM of SHK (Fig. 5 B and C). On the other hand, TNF (formerly known as TNF-α) was dramatically increased at 10 μM of SHK and decreased at 1 μM of SHK treatment (Fig. 6 B and C).

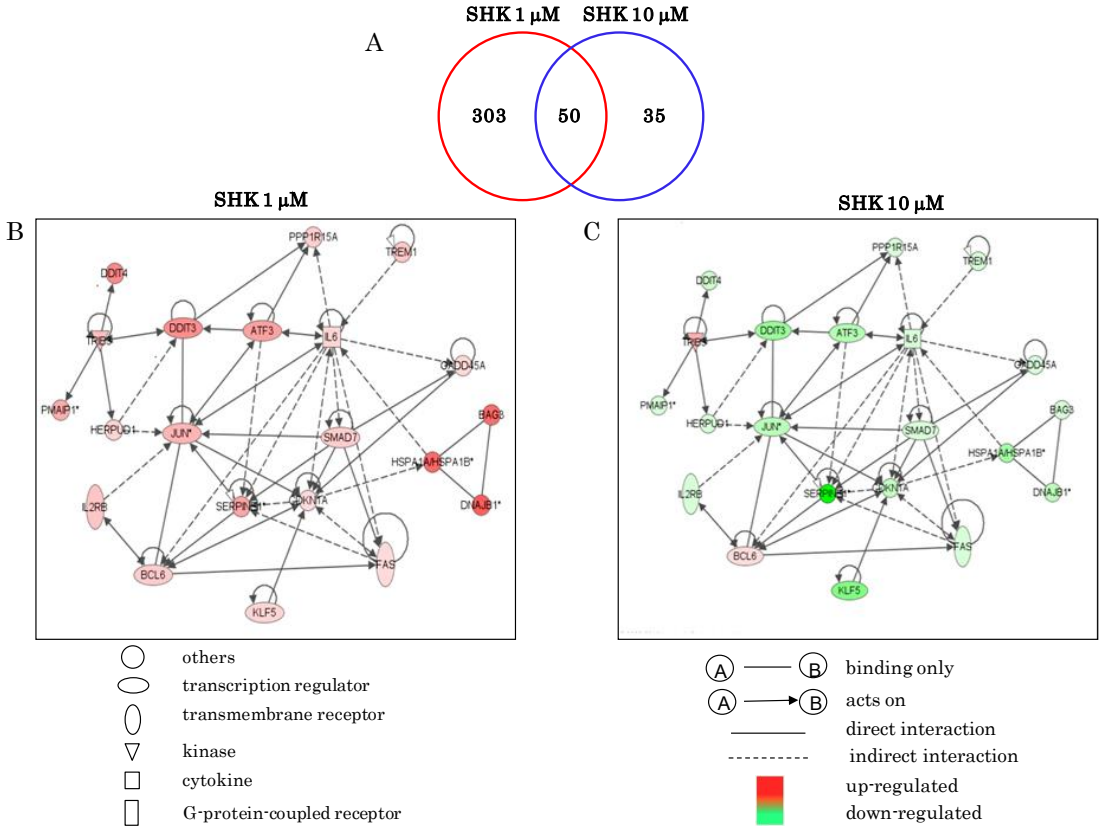

Figure 5. Changes in gene networks induced by SHK. U937 cells treated with 1 and 10 μM of SHK for 3 h, GeneChip® analysis was performed. The changes of the genes by SHK were analyzed using Ingenuity Pathways Analysis tools. The networks were displayed graphically as nodes (genes or proteins) and edges (the biological relationships between the nodes). The colors of the nodes indicate the expression level of the genes. Nodes and edges are displayed by various shapes and labels that represent the functional class of genes and the nature of the relationship between the nodes, respectively. (A) Venn diagram of the up-regulated genes by ≥2.5-fold in cells exposed to 1 and 10 μM of SHK. (B) Up-regulated genes with 1 μM of SHK. (C) Regulation of similar genes as shown in A, with 10 μM of SHK.

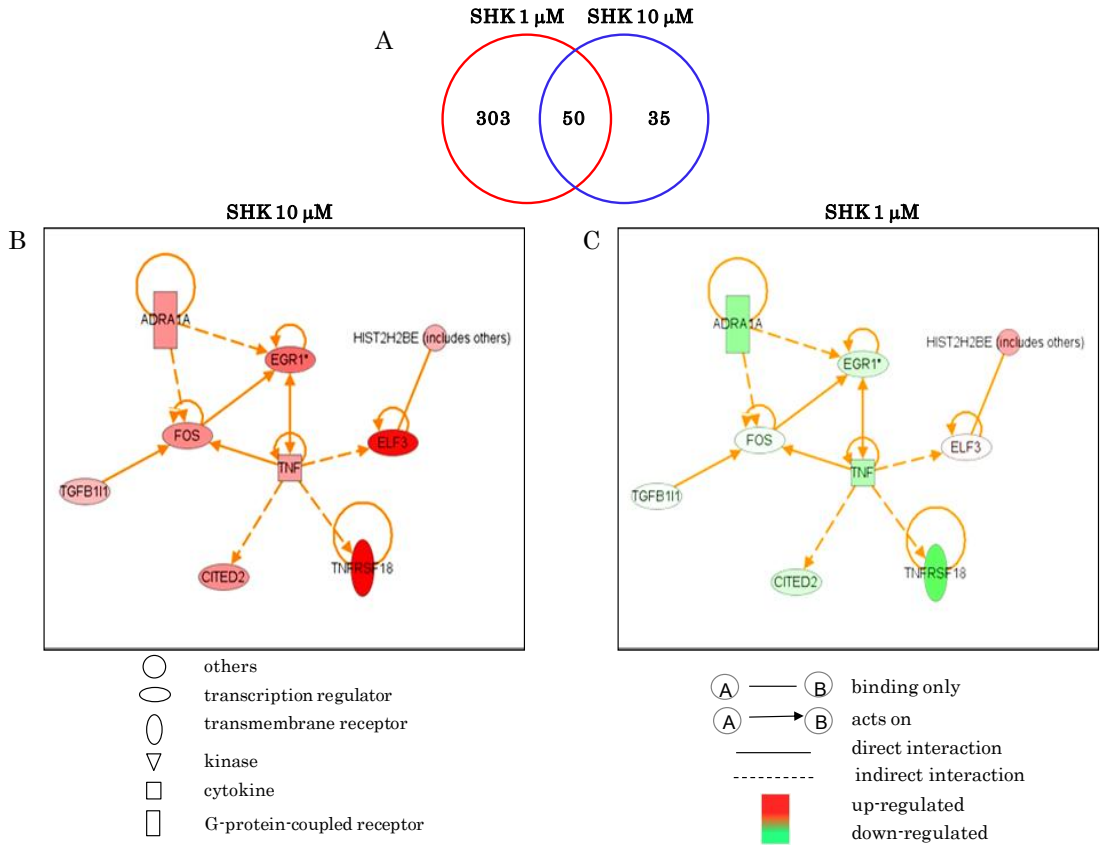

Figure 6. Changes in gene networks induced by SHK. U937 cells treated with 1 and 10 μM of SHK for 3 h, GeneChip® analysis was performed. The changes of the genes by SHK were analyzed using Ingenuity Pathways Analysis tools. The networks were displayed graphically as nodes (genes or proteins) and edges (the biological relationships between the nodes). The colors of the nodes indicate the expression level of the genes. Nodes and edges are displayed by various shapes and labels that represent the functional class of genes and the nature of the relationship between the nodes, respectively. (A) Venn diagram of the up-regulated genes by ≥2.5-fold in cells exposed to 1 and 10 μM of SHK. (B) Up-regulated genes with 10 μM of SHK. (C) Regulation of similar genes as shown in A, with 1 μM of SHK.

4.6. Verification of differentially expressed genes

To verify the microarray results, real-time qPCR assay was performed. The expression levels of four selected genes were comparable to those determined by microarray analysis; the expression levels of ATF3, DDIT3 were significantly increased at 1 μM of SHK and TNF was significantly increased at 10 μM of SHK for 3 h. In addition, we verified their protein expression by Western blot analysis (Fig. 7). These results are very similar to those of the microarray experiments.

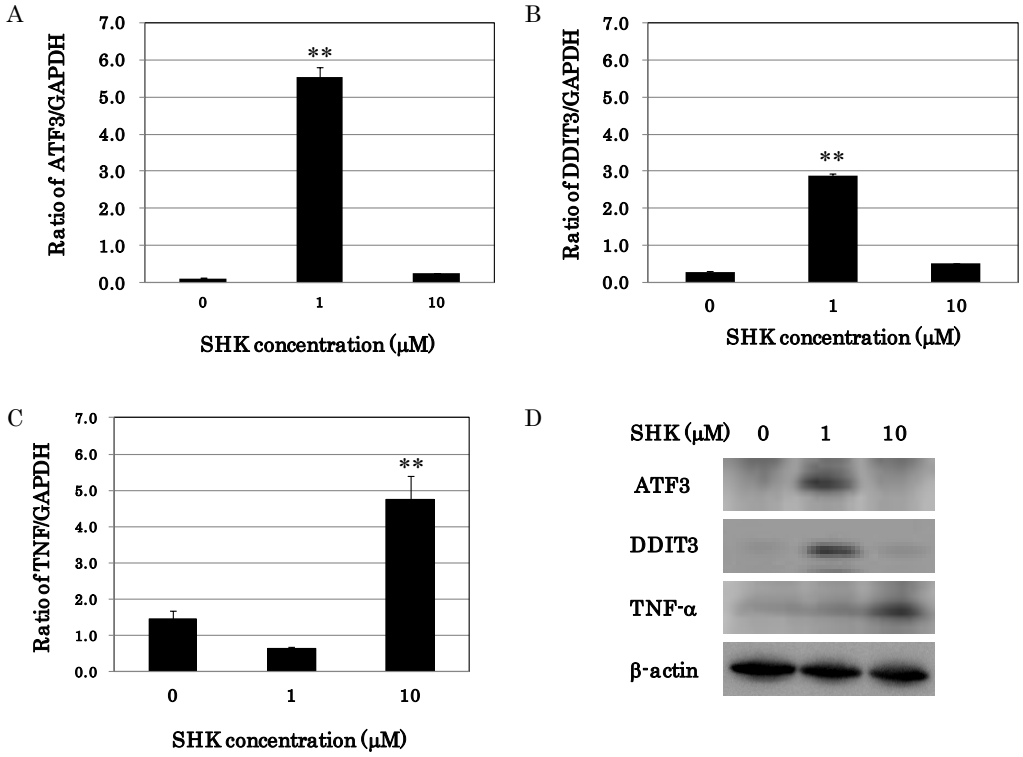

Figure 7. Verification of microarray results by real-time qPCR and Western blot analysis. U937 cells were treated with 1 and 10 μM of SHK and then incubated at 37˚C for 3 h and then real-time qPCR assay was performed. (A) ATF3. (B) DDIT3. (C) TNF. Each mRNA expression level was normalized to GAPDH expression level. The results are presented as the means ± SD (n = 4). **$p < 0.01$ denotes a mean significantly different from control. (D) The cells were treated with 1 and 10 μM of SHK and then incubated at 37˚C for 6 h, and protein expression of ATF3, DDIT3, and TNF-α was determined by Western blot analysis. Representative results from three independent experiments are shown.

5. Discussion

In this study, we were able to demonstrate that both apoptosis and necroptosis can be induced in U937 cells after treatment with different concentrations of SHK. It has been reported that SHK induces apoptosis in human bladder cancer T24 cells [24] and HeLa cells [25]. In both cancer cells caspase-3 plays a key role in the apoptosis induction. Recently, it has been reported that SHK also induces necroptosis in HL-60 cells, and this cell death is associated with change of mitochondrial membrane permeability [7].

Excessive intracellular ROS generation is known to induce mitochondrial dysfunction and subsequently release cytochrome c from mitochondria into the cytosol, which in turn activates the caspase cascade. Activation of the caspase cascade will execute apoptosis and is also considered as a characteristic feature that distinguishes between apoptotic and non-apoptotic cell death [26,27]. In the present study, low dose of SHK has been found to induce DNA fragmentation, increases in intracellular ROS generation, loss of MMP (Fig. 1).

SYTOX® Green is impermeant to live cells and cells undergoing apoptosis, and it is a useful indicator for necrotic cell death [28]. SHK-induced non-apoptotic cell death was determined by SYTOX® Green at 10 μM of SHK. Nec-1 significantly suppressed SHK-induced SYTOX® Green stained cells (Fig. 2C). These results clearly indicate that SHK-induced necroptosis at high concentration in U937 cells.

Oxidative stress is not only important in apoptosis, but also involved in the necroptosis signal transduction [29]. In the present study, cell impermeable GSH inhibits both apoptosis (Fig. 3B) and necroptosis at higher concentrations (data not shown). It suggests that SHK is able to interact with GSH outside of cells and that this interaction that depletes intracellular GSH is associated with SHK-induced cell death. This is consistent with another finding that the pre-treatment of cell membrane permeable GSH-MEE not only inhibit 1 μM of SHK-induced apoptosis, but also convert 10 μM of SHK-induced necroptosis to apoptosis (Fig.3A). Reduced GSH, is the most prevalent cellular thiol that protect cells from oxidative stress by playing an essential role in preserving a reduced intracellular environment. It is considered that the higher dose of SHK results in a more severe depletion of GSH and oxidative stress. We conclude that intracellular GSH was depleted by SHK dose dependently; massive oxidative stress induced by 10 μM of SHK causes breaks down of mitochondria, inhibit apoptosis and lead to necroptotic cell death.

Mitochondrial membrane permeabilization is tightly regulated by complex interaction of Bcl-2 family proteins in the apoptosis process [12], in contrast of that necroptosis is linked to rapid mitochondrial dysfunction without activation of caspase

cascade [30,31]. Bid is a pro-apoptotic Bcl-2 family member containing a BH3 domain only, which can be cleaved by caspase-8, and the cleaved Bid translocates to mitochondria and causes the induction of cytochrome c [32]. In addition, up-regulation of Noxa that causes mitochondrial membrane permeabilization and cytochrome c release is a promising key mechanism underlying potent apoptosis [33]. In this study, increases in the expression of tBid and Noxa were observed and this evidence indicates that Bid is cleaved and activated by SHK at low dose (Fig. 4C). Therefore, these findings indicate that the low dose of SHK induced apoptosis through mitochondria-caspase dependent pathway. Interestingly, under 10 μM of SHK treatment, cytochrome c was released from mitochondria in increased amount compared to that under 1 μM of SHK (Fig. 4A), without any changes of those BH3 domain only proteins observed in 1 μM of SHK (Fig. 4C). Therefore, these data suggest that 10 μM of SHK induce increase necroptosis without any conventional apoptotic signal transduction.

In the present study, GeneChip® analysis data also support the hypothesis. CREB/ATF family of transcription factors and Ap-1 pathways were significantly up-regulated at 1 μM of SHK (Fig. 5A). ATF3 is a member of CREB/ATF family, is able to both homodimerize and heterodimerize with other basic-region leucine zipper transcription factors, such as CHOP/DDIT3, JUN [34]. DDIT3 is usually expressed at undetectable levels and its expression is induced by cellular stress [35]. ATF3 with DDIT3 regulate gene expression, important to cellular repair and apoptosis. It has been reported that loss of ATF3 function, reduce stress-induced expression of PPP1R15A, is correlated with DNA damage and growth arrest induced apoptosis [36]. In addition, JUN is the most important component of Ap-1 transcription factors. It has been well accepted that JUN regulates cell proliferation, transformation and apoptosis. JUN dependent pro-apoptotic protein FasL has also been reported in several experimental systems [37]. FAS trigger apoptosis through FADD-mediated recruitment and activation of caspase-8 [11]. FAS-induced apoptosis requires amplification through proteolytic activation of the pro-apoptotic Bcl-2 family member Bid [38]. However,

those genes were clearly down-regulated by 10 μM of SHK, it indicate that ATF3, DDIT3, JUN and FAS are associated with low dose SHK-induced apoptosis, and lack of these apoptotic signal transduction at 10 μM of SHK lead the cell death to necroptosis.

On the other hand, significant increase of TNF expression is one of the most remarkable events at 10 μM of SHK treatment. TNF encodes a multifunctional pro-inflammatory cytokine that belongs to the TNF super family. This cytokine is mainly secreted by macrophages and is involved in the regulation of a wide spectrum of biological processes, such as cell proliferation, differentiation, and cell death. TNF is able to trigger both apoptosis and necroptosis [13]. It has been demonstrated that TNF stimulus are able to execute necroptosis when the apoptosis pathway is inhibited or inactive. Ubiquitination of RIP1 and alternative activation of caspase-8 is an important factor for signaling towards induction of apoptosis, conversely, RIP1-RIP3 complex has a central role in necroptosis [15-17]. In agreement with that 10 μM of SHK induced necroptosis accompanied with increases in TNF expression (Fig. 6A) without caspase-8 activation (Fig. 4B).

Microarray analysis showed the up-regulation of cytoprotective genes such as BAG3, DNAJB1 and HSPA1A/HSPA1B [39] at low dose of SHK (Fig. 5A). Previously, our group identified HSPA1A and DNAJB1 (Hsp40 homologs) being up-regulated by SHK without induction of cell death [40]. We consider that the expression of the genes is a response to the SHK-induced oxidative stress. However, the oxidative stress induced by SHK might overcome the cytoprotective effects of the BAG3 or the HSP-related genes, and thus the cells fate to the cell death.

On the basis of these findings, we conclude that (1) Low dose SHK induces apoptosis via mitochondria caspase dependent pathway; (2) High dose SHK induces necroptotic cell death by up-regulation of TNF expression and lack of activation in the downstream components of apoptosis; (3) Depletion of intracellular GSH and oxidative stress are involved in the cell death induced by SHK. To identify which gene is the key to determine the cell fate to necroptosis or apoptosis, further investigation is

under progress.

6. References

[1] L.A. Brigham, P.J. Michaels, H.E. Flores, Cell-specific production and antimicrobial activity of naphthoquinones in roots of Lithospermum erythrorhizon, Plant Physiol. 119 (1999) 417-428.

[2] X. Chen, L. Yang, N. Zhang, J.A. Turpin, R.W. Buckheit, C. Osterling, J.J Oppenheim, O.M. Howard, Shikonin, a component of chinese herbal medicine, inhibits chemokine receptor function and suppresses human immunodeficiency virus type 1, Antimicrob Agents Chemother. 47(2003)2810-2816.

[3] X. Chen, L. Yang, J.J. Oppenheim, M.Z. Howard, Cellular pharmacology studies of shikonin derivatives, Phytother Res. 16(2002) 199-209

[4] S. Hashimoto, M. Xu, Y. Masuda, T. Aiuchi, S. Nakajo, J. Cao, M. Miyakohi, Y. Ida, K. Nakaya, β-Hydroxyisovalerylshikonin inhibits the cell growth of various cancer cell lines and induces apoptosis in leukemia HL-60 cells through a mechanism different from those of Fas and etoposide, J. Biochem. 125 (1999) 17-23.

[5] X. Mao, C.R. Yu, W.H. Li, W.X. Li, Induction of apoptosis by shikonin through a ROS/JNK mediated process in Bcr/Abl–positive chronic myelogenous leukemia (CML) cells, Cell Res. 18 (2008) 879-888.

[6] I.C. Chang, Y.J. Huang, T.I. Chiang, C.W. Yeh, L.S. Hsu, Shikonin induces apoptosis through reactive oxygen species/extracellular signal-regulated kinase pathway in osteosarcoma cells, Biol. Pharm. Bull. 33 (2010) 816-824.

[7] W. Han, J. Xie, L. Li, Z. Liu, X. Hu, Necrostatin-1 reverts shikonin-induced necroptosis to apoptosis, Apoptosis 14 (2009) 674-686.

[8] J.F. Kerr, A.H. Wyllie, A.R. Currie, Apoptosis: a basic biological phenomenon with wide-ranging implications in tissue kinetics, Br. J. Cancer 26 (1972) 239-257.

[9] K.M. Hajra, J.R. Liu, Apoptosome dysfunction in human cancer, Apoptosis 9 (2004)

691-704.

[10] J.T. Opferman, S.J. Korsmeyer, Apoptosis in the development and maintenance of the immune system, Nat. Immunol. 4 (2003) 410-415.

[11] H. Wajant, The Fas signaling pathway: more than a paradigm, Science 296 (2002) 1635-1636.

[12] Y. Tsujimoto, S. Shimizu, Bcl-2 family: life-or-death switch, FEBS Lett. 466 (2000) 6-10.

[13] S.M. Laster, J.G. Wood, L.R. Gooding, Tumor necrosis factor can induce both apoptic and necrotic forms of cell lysis, J. Immunol. 141 (1988) 2629–2634.

[14] S.W. Tait, D.R. Green, Caspase-independent cell death: leaving the set without the final cut, Oncogene 27 (2008) 6452-6461.

[15] A. Degterev, J. Hitomi, M. Germscheid, I.L. Ch'en, O. Korkina, X.Teng. G.D. Cuny, C. Yuan, G. Wagner, S.M. Hedrick, S.A. Gerber, A. Lugovskoy, J. Yuan, Identification of RIP 1 kinase as a specific cellular target of necrostatins, Nat. Chem. Biol. 4 (2008) 313-321.

[16] W. Declercq, T. Vanden Berghe, P. Vandenabeele, RIP kinases at the crossroads of cell death and survival, Cell 138 (2009) 229-232.

[17] Y.S. Cho, S. Challa, D. Moquin, R. Genga, T.D. Ray, M. Guildford, F.K. Chan, Phosphorylation-driven assembly of the RIP1-RIP3 complex regulates programmed necrosis and virus-induced inflammation, Cell 137 (2009) 1112-1123.

[18] Y. Zhu, P.M. Carvey, Z. Ling, Age-related changes in glutathione and glutathione-related enzymes in rat brain, Brain Res. 1090 (2006) 35–44.

[19] K.S. Sellins, J.J. Cohen, Gene induction by gamma-irradiation leads to DNA fragmentation in lymphocytes, J. Immunol. 139 (1987) 3199-3206.

[20] V. Petronilli, D. Penzo, L. Scorrano, P. Bernardi, F. Di Lisa, The mitochondrial permeability transition, release of cytochrome c and cell death, J. Biol. Chem. 276 (2001)12030-12034.

[21] Z.G. Cui, T. Kondo, R. Ogawa, L.B. Feril Jr, Q.L. Zhao, S. Wada, T. Arai, K.

Makino, Enhancement of radiation-induced apoptosis by 6-formylpterin, Free Radic. Res. 38 (2004) 363-373.

[22] Y. Tabuchi, I. Takasaki, T. Kondo, Identification of genetic networks involved in the cell injury accompanying endoplasmic reticulum stress induced by bisphenol A in testicular Sertoli cells, Biochem. Biophys. Res. Commun. 345 (2006) 1044-1050.

[23] T. Hori, T. Kondo, Y. Tabuchi, I. Takasaki, Q.L. Zhao, M. Kanamori, T. Yasuda, T. Kimura, Molecular mechanism of apoptosis and gene expressions in human lymphoma U937 cells treated with anisomycin, Chem. Biol. Interact. 172 (2008) 125-140.

[24] C.C. Yeh, H.M. Kuo, T.M. Li, J.P. Lin, F.S. Yu, H.F. Lu, J.G. Chung, J.S. Yang, Shikonin-induced apoptosis involves caspase-3 activity in a human bladder cancer cell line (T24), In Vivo. 21 (2007) 1011-1020

[25] Z. Wu, L.J. Wu, L.H. Li, S. Tashiro, S. Onodera, T. Ikejima, Shikonin regulates HeLa cell death via caspase-3 activation and blockage of DNA synthesis J. Asian. Nat. Prod Res. 6 (2004) 155-166.

[26] M. Ott, V. Gogvadze, S. Orrenius, B. Zhivotovsky, Mitochondria, oxidative stress and cell death, Apoptosis 12 (2007) 913-922.

[27] H. Li, J. Yuan, Deciphering the pathways of life and death, Curr. Opin. Cell Biol. 11 (1999) 261-266.

[28] H. Shibata, T. Ichikawa, K. Nakao, H. Miyaaki, S. Takeshita, M. Akiyama, S. Miuma, H. Yamasaki, K. Eguch, A high glucose condition sensitizes human hepatocytes to hydrogen peroxide-induced cell death, Mol. Med. Rep. 1 (2008) 379-385.

[29] K.J. Song, Y.S. Jang, Y.A. Lee, K.A. Kim, S.K. Lee, M.H. Shin, Reactive oxygen species-dependent necroptosis in Jurkat T cells induced by pathogenic free-living Naegleria fowleri, Parasite Immunol. 33 (2011) 390-400

[30] J.Y. Kim, Y.J. Kim, S. Lee, J.H. Park, Bnip3 is a mediator of TNF-induced necrotic cell death, Apoptosis 16 (2011) 114-126.

[31] N. Li, L. Wang, C. Mo, W. Zhang, J. Li, Z. Liao, X. Tang, H. Xiao, D-galactose induces necroptotic cell death in neuroblastoma cell lines, J. Cell Biochem. 112 (2011) 3834-3844.

[32] X. Luo, I. Budihardjo, H. Zou, C. Slaughter, X. Wang, Bid, a Bcl2 interacting protein, mediates cytochrome c release from mitochondria in response to activation of cell surface death receptors, Cell 94 (1998) 481-490.

[33] C. Ploner, R. Kofler, A. Villunger Noxa: at the tip of the balance between life and death, Oncogene 27 (2008) S84-S92.

[34] S.H. Lee, J.H. Bahn, N.C. Whitlock and S.J. Baek, Activating transcription factor 2 (ATF2) controls tolfenamic acid-induced ATF3 expression via MAP kinase pathways, Oncogene 29 (2010) 5182-5192.

[35] P.E. Lovat, S. Oliverio, M. Panalli, M. Corazzari, C. Rodolfo, F. Bernassola, K. Aughton, M. Maccarrone, Q.D. Hewson, A.D. Pearson, G. Melino, M. piacentini, C.P. Redfern, GADD153 and 12-lipoxygenase mediate fenretinide-induced apoptosis of neuroblastoma, Cancer Res. 62(2002) 5158-5167.

[36] A.V. Grishin, O. Azhipa, I. Semenov, S.J. Corey, Interaction between growth arrest-DNA damage protein 34 and Src kinase Lyn negatively regulates genotoxic apoptosis, Proc. Natl. Acad. Sci. U. S. A. 98 (2001) 10172-10177.

[37] D. Holzberg, C.G. Knight, O. Dittrich-Breiholz, H. Schneider, A. Dörrie, E. Hoffmann, K. Resch, M. Kracht, Disruption of the c-JUN-JNK complex by a cell-permeable peptide containing the c-JUN delta domain induces apoptosis and affects a distinct set of interleukin-1-induced inflammatory genes, J. Biol. Chem. 278 (2003) 40213-40223.

[38] G. Denecker, D. Vercammen, M. Steemans, T. Vanden Berghe, G. Brouckaert, G. Van Loo, B. Zhivotovsky, W. Fiers, J. Grooten, W. Declercq, P. Vandenabeele, Death receptor-induced apoptotic and necrotic cell death: differential role of caspases and mitochondria, Cell Death Differ. 8 (2001) 829-840.

[39] Y. Furusawa, Y. Tabuchi, S. Wada, Takasaki I, K. Ohtsuka and T. Kondo, Identification of biological functions and gene networks regulated by heat stress

in U937 human lymphoma cells, Int. J. Mol. Med. 28 (2011) 143-151.

[40] K. Ahmed, Y. Furuawa, Y. Tabuchi, H.F. Emam, J.L. Piao, M.A. Hassan, T. Yamamoto, T. Kondo, M. Kadowaki, Chemical inducers of heat shock proteins derived from medicinal plants and cytoprotective genes response, Int. J. Hyperthermia 28 (2012) 1-8.

7. Acknowledgments

I would like to express my sincere gratitude to Professor Takashi Kondo, Department of Radiological Sciences, Graduate School of Medicine Pharmaceutical Sciences, University of Toyama, for his Support, supervision, encouragement, inspiring guidance and trust during my study period.

Thanks to all my professors and colleagues of the department of radiological science who were so kind and helpful to me all those years.

Jin-Lan Piao

Department of Radiological Science

Graduate School of Medicine and Pharmaceutical Science

University of Toyama